Jefferson Lab PAC13
Proposal Cover Sheet

This document must be received by close of business Thursday, **December 18, 1997** at:

Jefferson Lab
User Liaison Office,
Mail Stop 12B
12000 Jefferson Avenue
Newport News, VA
23606

Experimental Hall: C

Days Requested for Approval: 17

☒ **New Proposal Title:** Studying the Internal Small-distance Structure of Nuclei via the Triple Coincidence (e,ep+N) Measurement

☐ **Update Experiment Number:**

☐ **Letter-of-Intent Title:**

(Choose one)

Proposal Physics Goals

Indicate any experiments that have physics goals similar to those in your proposal.

Approved, Conditionally Approved, and/or Deferred Experiment(s) or proposals:

Approved: E89-036 (Hall B), E97-011 (Hall A)

Contact Person

Name: Stephen A. Wood
Institution: Jefferson Laboratory
Address: Jefferson Laboratory, MS 12H
Address: 12000 Jefferson Avenue
City, State, ZIP/Country: Newport News, VA 23606
Phone: (757) 269-7367 **Fax:** (757) 269-5235
E-Mail: saw@jlab.org

JLab Use Only

Receipt Date: 12/18/97 PR 97-106

By: gp

BEAM REQUIREMENTS LIST

JLab Proposal No.: _____ Date: Dec 18, 1997

Hall: C Anticipated Run Date: _____ PAC Approved Days: _____

Spokesperson: E. Piasetzky (TAU) Hall Liaison: _____
Phone: 972-3-640-9428
E-mail: eip@tauphy.tau.ac.il
Contact Person: Stephen A. Wood (JLab), (757)269-7367, saw@jlab.org

List all combinations of anticipated targets and beam conditions required to execute the experiment. (This list will form the primary basis for the Radiation Safety Assesment Document (RSAD) calculations that must be performed for each experiment.)

Condition No.	Beam Energy (MeV)	Mean Beam Current (μA)	Polarization and Other Special Requirements (e.g., time structure)	Target Material (use multiple rows for complex targets — e.g., w/windows)	Material Thickness (mg/cm²)	Est. Beam-On Time for Cond. No. (hours)
1		10-100		C	0.2	100
2	4000	100		C	0.2	300

The beam energies, E_{Beam}, available are: $E_{Beam} = N \times E_{Linac}$ where N = 1, 2, 3, 4, or 5. E_{Linac} = 800 MeV, i.e., available E_{Beam} are 800, 1600, 2400, 3200, and 4000 MeV. Other energies should be arranged with the Hall Leader before listing.

HAZARD IDENTIFICATION CHECKLIST

JLab Proposal No.: _____ Date: Dec 18, 1997
(For CEBAF User Liaison Office use only.)

Check all items for which there is an anticipated need.

Cryogenics
- _____ beamline magnets
- ✓ analysis magnets
- ✓ target
  - type: LH_2
  - flow rate: _____
  - capacity: _____

Electrical Equipment
- _____ cryo/electrical devices
- _____ capacitor banks
- ✓ high voltage
- _____ exposed equipment

Extra 50 channels of PMT HV

Radioactive/Hazardous Materials
List any radioactive or hazadorous/ toxic materials planned for use:

Pressure Vessels
- _____ inside diameter
- _____ operating pressure
- _____ window material
- _____ window thickness

*

Flammable Gas or Liquids
- type: _____
- flow rate: _____
- capacity: _____

*

Drift Chambers
- type: _____
- flow rate: _____
- capacity: _____

*

Other Target Materials
- ___ Beryllium (Be)
- ___ Lithium (Li)
- ___ Mercury (Hg)
- ___ Lead (Pb)
- ___ Tungsten (W)
- ___ Uranium (U)
- ___ Other (list below)

1mm Carbon

Vacuum Vessels
- _____ inside diameter
- _____ operating pressure
- _____ window material
- _____ window thickness

*

Radioactive Sources
- _____ permanent installation
- ✓ temporary use
- type: ^{228}Th for scintillator
- strength: calibration

Large Mech. Structure/System
- _____ lifting devices
- _____ motion controllers
- _____ scaffolding or
- _____ elevated platforms

Shielding for third arm

Lasers
- type: _____
- wattage: _____
- class: _____

Installation:
- _____ permanent
- _____ temporary

Use:
- _____ calibration
- _____ alignment

Hazardous Materials
- ___ cyanide plating materials
- ___ scintillation oil (from)
- ___ PCBs
- ___ methane
- ___ TMAE
- ___ TEA
- ___ photographic developers
- ___ other (list below)

_____

_____

*

General:

Experiment Class:
- ✓ Base Equipment
- _____ Temp. Mod. to Base Equip.
- _____ Permanent Mod. to Base Equipment
- _____ Major New Apparatus

Other: Third arm of plastic counters for neutron detection

* Standard Hall C equipment

LAB RESOURCES LIST

JLab Proposal No.: _____ Date December 18, 1997
(For JLab ULO use only.)

List below significant resources — both equipment and human — that you are requesting from Jefferson Lab in support of mounting and executing the proposed experiment. Do not include items that will be routinely supplied to all running experiments such as the base equipment for the hall and technical support for routine operation, installation, and maintenance.

Major Installations *(either your equip. or new equip. requested from JLab)*

New Support Structures:

Data Acquisition/Reduction

Computing Resources:

New Software: Small change in Standard DAQ to read third arm information

Major Equipment

Magnets:

Power Supplies:

Targets:

Detectors: (1) Shielding for third arm: fixed position about 90° to beam

Electronics: (2) 50 signal cables from Hall to counting house

Computer Hardware: (3) ~ 50 TDC channels. ADC's optional

Other:

Other:

LAB RESOURCES LIST

JLab Proposal No.: _____ Date December 18, 1997
(For JLab ULO use only.)

List below significant resources — both equipment and human — that you are requesting from Jefferson Lab in support of mounting and executing the proposed experiment. Do not include items that will be routinely supplied to all running experiments such as the base equipment for the hall and technical support for routine operation, installation, and maintenance.

Major Installations *(either your equip. or new equip. requested from JLab)*

New Support Structures:

Data Acquisition/Reduction

Computing Resources:

New Software: Small change in Standard DAQ to read third arm information

Major Equipment

Magnets:

Power Supplies:

Targets:

Detectors: (1) Shielding for third arm: fixed position about 90° to beam

Electronics: (2) 50 signal cables from Hall to counting house

Computer Hardware: (3) ~ 50 TDC channels. ADC's optional

Other:

Other:

LAB RESOURCES LIST

JLab Proposal No.: _____ Date December 18, 1997
(For JLab ULO use only.)

List below significant resources — both equipment and human — that you are requesting from Jefferson Lab in support of mounting and executing the proposed experiment. Do not include items that will be routinely supplied to all running experiments such as the base equipment for the hall and technical support for routine operation, installation, and maintenance.

Major Installations *(either your equip. or new equip. requested from JLab)*

New Support Structures:

Data Acquisition/Reduction

Computing Resources:

New Software: Small change in Standard DAQ to read third arm information

Major Equipment

Magnets:

Power Supplies:

Targets:

Detectors: (1) Shielding for third arm: fixed position about 90° to beam

Electronics: (2) 50 signal cables from Hall to counting house

Computer Hardware: (3) ~ 50 TDC channels. ADC's optional

Other:

Other:

Studying the internal small-distance structure of nuclei via the triple coincidence $(e, ep + N)$ measurement

J. Alster, D. Ashery, L. Frankfurt, S. Malik and *E. Piasetzky (spokesperson)*
Tel Aviv University, Israel

W. Bertozzi (spokesperson), K. Fissum, J. Gao, S. Gilad, N. Liyanage,
D. Rowntree, J. Zhao and Z-Lu Zhou
MIT

B. Anderson, A. Baldwin, M. Manley, G. Petratos, D. Prout,
John Watson(spokesperson) and W-Ming Zhang
KSU

S. Danagulian, C. Jackson and R. Sawafta
North Carolina AT SU

S. Heppelmann and M. Strikman
PSU

R. Carlini, J. Dunne, R. Ent, A.F. Lung, D. Mack, J.H. Mitchell,
W.F. Vulcan and *S.A. Wood (spokesperson)*
Jefferson Laboratory

O.K. Baker, C.E. Keppel and L. Tang
Hampton University

N. Christensen
University of Auckland, New Zealand

K.Sh. Egiyan, G.V. Gavalian, H.G. Mkrtchyan, M.M. Sargsian and S.G. Stepanyan
Yerevan Physics Institute, Armenia

V. Nelyubin, V. Ryazanov, V. Tarakanov and M. Zhalov
Institute for Nuclear Physics, St.Petersburg, Russia

J. Templon
University of Georgia

ABSTRACT

We propose to measure the C(e,e'p+N) reaction in hall C. The two permanent magnetic spectrometers will be used to measure the (e,e'p) part of the reaction. We plan to add a third arm, consisting of a series of scintillation counters, to measure neutrons and protons in coincidence with the outgoing high momentum electron and proton.

We choose kinematical conditions that will allow us to determine the fraction of (e,e'p) events which are associated with NN short range correlations, as a function of the momentum of the proton in the nucleus. It will also allow us to compare between *pn* and *pp* correlated pairs in nuclei.

This proposal expands the existing limits to large Q^2, $x > 1$ and "exclusiveness" which were not covered by earlier data or other proposals to TJNAF. We will discuss the importance of these kinematical constraints for the identification of NN short range correlations in nuclei and how they may overcome the obstacles from final state interactions, meson exchange currents and resonance production.

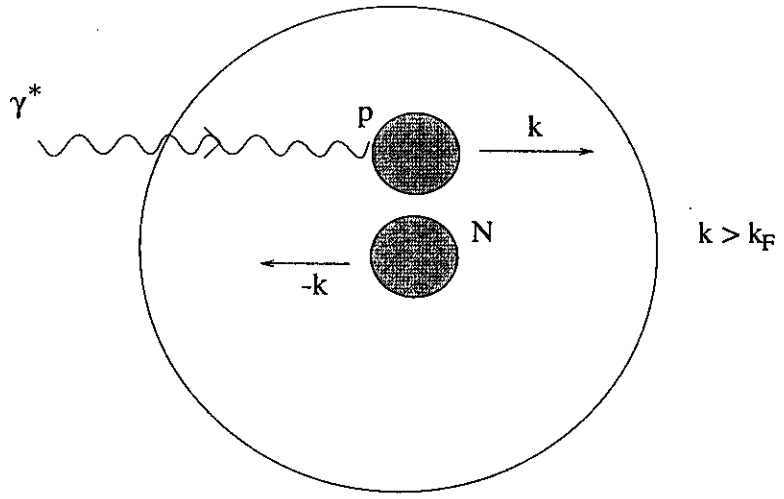

1 Introduction

1.1 Scientific background

Most nuclear properties can be described successfully within the single particle model. However, the simple picture breaks down when some detailed features are studied, especially in the extreme regions of the nuclear wave function. In recent years much attention has been paid to the role that two-nucleon correlations play in nuclei. Large high momentum tails in the nuclear spectral function were calculated with realistic potentials of two-and three-body interactions. A significant probability of NN correlations was predicted for light nuclei [1] for nuclear matter [2] and for an interpolation between these [3]. The field has been reviewed recently by Pandharipande et al. [4].

We will mention some experiments that addressed this issue. We will classify them by order of complexity, and by the kinematical parameters of the measurement. There are inclusive (e,e') experiments [5, 6] at high momentum transfers and $x > 1$. They obtained the momentum distribution of the nucleons in the nucleus in terms of the y-scaling variable. Relatively large high-momentum tails are observed. Theoretical models try to explain this by invoking short range correlations [7]. Others [8] explained the results in terms of final state interactions (FSI).

There are (e,e') measurements in the "dip" region, between the quasi-elastic peak and the delta region, at x$\leq$1 which show an anomalously large transverse cross section. This has been cited as evidence for NN correlations. [9, 10] and references in [10].

In the next order of complexity we mention the semi-exclusive (e,ep) experiments at small values of Q^2 and x$\leq$1 [11, 12, 13], One observes a depletion of spectroscopic strength which may be explained by nuclear correlations which push the nucleons to higher momentum states and high missing energies and are thus not visible at low momenta and low excitation energies [10]. The depletion can be as large as 35% [4]. Other (e,e'p) experiments [14, 15, 16], also at $x < 1$ show peaks at missing energies corresponding to the removal of two nucleons . There are two- nucleon knockout reactions (e, ed), (e, epp) and (e, epn) [17, 18, 19, 20] and real photon absorption $(\gamma, 2N)$ [21, 22]. In the above experiments the knocked out proton was detected in the forward direction relative to the photon momentum.

There are measurements of backward scattered protons from a variety of projectiles [23] as well as (e,e'p) experiments at $x \leq 1$ [24] and deep inelastic (ν,μ p) [25] scattering where backward going protons were observed in coincidence with a forward going particle, electron and muon, respectively. Correlations were claimed between the transferred energy and the momenta of the backward going protons. There is also evidence from pion absorption experiments [26] which have to take place on (at least) a couple of nucleons. Last but not least we mention the experiment (E850) at BNL which studied the reaction C(p,2p+n). The outgoing high energy protons were detected in coincidence with a relatively low energy neutron. This experiment will be discussed in section 1.3 and in the Appendix.

The SRC between two nucleons in nuclei are a very elusive feature in nuclear physics. Their identification by the above mentioned experiments at low energies, is very difficult because their signal is usually small compared to the single particle components. It is also difficult to separate SRC from meson exchange currents (MEC) and FSI. Most of the experiments were done at $x < 1$ which sets the kinematics close to the delta production region and/or at low Q^2 where MEC play a major role [16] and the FSI depend strongly on the proton energy.

1.2 Related experiments and proposals at TJNAF

Only recently a new generation of "kinematically complete" experiments which measure the scattered nucleon in coincidence with the correlated one were performed. This category includes (e,e'pN) measurements from MAMI and NIKHEF, (γ, NN) from TAGX and LEGS [21, 22]. Our proposed experiment belongs in that group of measurements but it expands the limits to large Q^2, $x > 1$ and the "exclusiveness" which were not covered by earlier data or other proposals to TJNAF . We will discuss, in section 2, the importance of these kinematical constraints for the identification of NN SRC in nuclei.

It is a natural next step in the order of measurements and proposals that were done or approved at TJNAF, both from the scientific interest and from technical aspects. We hope to benefit from the knowledge and experience accumulated in doing double coincidence experiments in halls A and C and to contribute some unique knowledge to our understanding of the nucleus at short distances.

In the following, we will place the proposal among other proposals at TJNAF, according to the Q^2 and X scales.

- $x > 1$

  Largely due to small cross sections the overall amount of data is still scarce at $x > 1$. There is an inclusive (e, e') experiment (Hall-C E 89-008 [27]) for studies in the $x > 1$ region. There is also a semi-inclusive (e,e'p) proposal approved for hall-A experiment E 97-011 [28] on ^3He and ^4He. This proposal is complementary to and augments the inclusive (e, e') and the semi-inclusive (e,e'p) proposals. The (e, e') will supply important information on the high momentum components in nuclei without information about the excitation of the residual nucleus. The semi-inclusive measurements contribute to our understanding of the microscopic origin of the high momentum tail by studying the spectral function as a function of p_m and E_m. The proposed triple coincidence experiment will allow us to study the decay function which is also a function of the momentum of the spectator nucleon. This is a much tighter measurement of the SRC contribution as we will discuss in detail. We propose to measure the contribution of 2N SRC to the high momentum tail as a function of that momentum. Data of this kind do no yet exist.

- Large Q^2

Experiment NE18 was a breakthrough in the Q^2 range that was used. Earlier (e,e'p) measurements were limited to Q^2 well below 1 $(GeV/c)^2$ and NE18 opened up a new front at several $(GeV/c)^2$. The proposed experiment provides a similar breakthrough for the more exclusive triple coincidence measurements. Data from NIKHEF and MAMI are limited to a small fraction of 1 $(GeV/c)^2$ and our measurement will open up a new domain above 2 $(GeV/c)^2$, about two orders of magnitude higher than any other data. The importance of large Q^2 to nail down the particular contribution from NN SRC will be discussed, in detail, further on.

- Exclusiveness.

  This is the first proposal to do a triple coincidence experiment in hall C. There are no data or approved proposals to do such an exclusive measurement in hall A or hall C. To the best of our knowledge there is no new competing proposal to do so. The low cross sections we intend to measure (at the level of pb/sr^2MeV) require the superior luminosities of one of these halls.

  Similar studies of SRC are planned [29, 30] in hall B using the reaction (e, e', pN) in complementary kinematical regions, mainly $x < 1$ (see also Refs.[31, 32]).

1.3 $A(p, 2p + n)$ measurements at BNL: data and plans

The reaction $A(p, 2p + n)$ was measured by us at BNL (E850) at beam momemta of 5.9 and 7.5 $(GeV/c)^2$. We established the quasi-elastic character of the reaction in a kinematically complete measurement. The neutron momentum was measured in triple coincidence with the two emerging high energy protons. We found a correlation between the momenta of the neutron and the struck target proton. The events were associated with the high momentum components of the nuclear wave function. The details are given in an appendix.

Based on our results from the (p,2p+n) reaction, we are encouraged to embark on a similar project with the electron probe. **Hopefully, with those mesurements, together with the data we wish to collect at TJNAF, we will be able to establish a unified description of SRC in nuclei.**

1.4 Proposed $A(e, ep + N)$ measurement at TJNAF

In many aspects, the electron-nucleus interaction is better understood than the nucleon-nucleus interaction. The electromagnetic interaction is weak compared to the hadronic one, and hence electrons probe the entire volume of the nucleus while hadrons tend to interact on the nuclear surface.

We propose to measure SRC at TJNAF in a quite similar way to that described in the previous section for the hadron-nucleus reaction. The proposed experiment will be significantly more precise in determining the quasi-elastic nature of the reaction and will have much better statistics than the experiment at BNL. There are several excellent

setups at the laboratory for measuring (e,e'p) scattering. For our main effort, we plan to add a third arm consisting of a series of counters to measure neutrons and protons in coincidence with the outgoing high momentum electron and proton. Just as for the (p,2p+n) reaction we will measure the full kinematics of the (e,e'p) reaction, but with much higher accuracy enabled by the TJNAF facilities. We can then extract the momentum of the struck proton. We will also measure the momentum and direction of an additional neutron or proton in coincidence with the outgoing e and p. **This will allow us to measure the fraction of (e,e'p) events in which NN correlated nucleons are observed, as a function of the initial momentum of the proton in the nucleus.** It will also allow us to compare between *pn* and *pp* correlated pairs in nuclei. We could not measure that ratio in the (p,2p+p) experiment because the targets were too thick and the low energy proton would loose a large amount of energy on its way out.

We will choose kinematical setups that select scattering from protons above the Fermi sea ($p_m > k_F$). We will use electron beams of 4 GeV (and above, if available), large momentum transfers in the region of $Q^2 = 2 - 3(GeV/c)^2$ and missing energy in the region of $E_m = p_m^2/2m$. These conditions will minimize the contributions from FSI and MEC. Details of the kinematics and the experimental setup will be given in sections 2 and 3 of this proposal.

Why measure both neutrons and protons in the third arm ? It is clear that one of the real exciting aspects of studying NN SRC is to understand it's isospin dependence. There are data on (γ, pp) and (γ, pn) [21, 22] and the ratio between the two cross sections. However the measurements with real photons measure only the transverse amplitudes whereas with virtual photons one can study the longitudinal amplitude as well (depending on the electron scattering angle). Also, FSI may play a significant role in those data. Thus, the ratio between the SRC *np* and *pp* pair contributions is not well known and is one of the expected outcomes of the proposed measurement

We measure at two Q^2 values, in order to ensure that we identify correctly the QE (e,e'p) character of the process. If our hypothesis and procedures are correct the two measurements should scale according to the free ep−− >ep process.

2 $^{12}C(e, ep + N)$ measurements at TJNAF

2.1 Kinematical characteristics of NN SRC

One of the main consequences of the short range nature of a NN interaction is the strong correlation between *the momenta* of the correlated nucleons. Thus, for a pair at rest, when knocking out one of the nucleons, the second (spectator) nucleon will have a momentum (p_s) which is balanced with the missing momentum of the knocked out nucleon: ($\vec{p}_s \approx -\vec{p}_m$). Since SRC will exist predominantly in the high momentum tail of the nuclear wave function, such a spectator should have a large p_s , $p_s \geq k_F \approx 250\ MeV/c$. See Fig. 6 for illustration.

Fig. 7 shows the dominant process we wish to look for and defines the kinematical variables. We discuss the quasi-free break-up reaction of the pair at rest and we denote the pair, at rest in the nucleus, as d (deuteron):

$$e + d \rightarrow e' + p + n \tag{1}$$

The kinematical conditions of the quasi-elastic reaction sets:

$$(q + p_d - p_f)^2 = m^2 \tag{2}$$

where $q = (q_0, \vec{q})$, $p_d = (m_d, \vec{0})$ and $p_f = (E_f, \vec{p}_f)$ are the four-momenta of the transfered momentum, the target pair and the detected final nucleon, respectively. ¿From the (e,e') information we determine the missing momentum as $\vec{p}_m = \vec{p}_f - \vec{q}$ and the missing energy as $E_m = q_0 - (E_f - m)$. ¿From eq.(2) we obtain the following relation between missing momentum and energy:

$$E_m = \sqrt{m^2 + p_m^2} + m - m_D \approx \frac{p_m^2}{2m} \tag{3}$$

Thus in the breakup of a pair there is a strong correlation between the measured missing momentum p_m and the missing energy E_m.

In terms of the decay function we discuss in detail in the next section , we concentrate on:

$$D(E_m = p_m^2/2m, p_m > k_F, \vec{p}_s = -\vec{p}_m) \tag{4}$$

2.2 Description of the $(e, ep + N)$ reaction

The cross section for the reaction when a proton is knocked out of the nucleus and a spectator nucleon in the final state is detected in coincidence with the scattered electron and proton, can be represented within the plane wave impulse approximation , as follows:

$$\frac{d\sigma}{dE' d\Omega_e d^3(p_f/E_f)(d^3p_s/Es)} = K_d \sigma_{ep}(Q^2, \epsilon, E_m, p_m) \cdot D(E_m, \vec{p}_m, \vec{p}_s). \tag{5}$$

The decay function D represents the joint probability to find inside the nucleus, a nucleon with missing momentum $p_m(p_{m-})$ and missing energy $E_m(p_{m+})$ and where the residual nuclear state contains the spectator nucleon with momentum $\vec{p}_s(p_{s\pm}, \vec{p}_t)$. Any four-momentum k can be represented as $k \equiv k(k_+, k_-, k_t)$ where $k_\pm = k_0 \pm k_z$, where the z and t components are defined along the direction and perpendicular to the direction of the transfered momentum (virtual photon momentum) $\vec{q}$, respectively. Using the above definitions, we introduce the light-cone components of the missing momenta as $p_{m+} \equiv p_{f+} - q_+ = m - E_m + p_{mz}$ and $p_{m-} = p_{f-} - q_- = m - E_m - p_{mz}$. With the light cone momenta $p_{m\pm}, p_{s\pm}$ representation, we write:

$$\frac{d\sigma}{dE' d\Omega_e d^3(p_f/E_f)(d^3p_s/Es)} = K_d \sigma_{ep}(Q^2, \epsilon, p_{m+}, p_{m-}) \cdot D(p_{m+}, p_{m-}, \vec{p}_{mt}, p_{s-}, \vec{p}_{st}). \quad (6)$$

where K_d is the kinematic factor, $\epsilon = [1 + 2\frac{q^2}{Q^2} tan^2(\theta_e/2)]^{-1}$ and σ_{ep} describes the electron scattering on an off-shell proton.

The decay function is related to the spectral function of $(e, e'p)$ reaction in the following way:

$$\int D(E_m, \vec{p}_m, \vec{p}_s) d^3p_s = S(E_m, \vec{p}_m) \quad (7)$$

or

$$\int D(p_{m+}, p_{m-}, \vec{p}_{mt}, p_{s-}, \vec{p}_{st}) d^2p_{st} dp_{s-} = S(p_{m+}, p_{m-}, \vec{p}_{mt}) \quad (8)$$

The decay function defines the quantities which can be studied experimentally by a triple coincidence measurement.

2.3 Suppression of competing effects.

The interpretation of existing low energy electron scattering data in terms of SRC has been plagued by contributions from meson exchange currents and final state interactions whose importance depends on the transfered momentum and kinematical conditions. In this section we discuss how we choose the kinematics that minimize these effects. We discuss the relation of high momentum transfer to FSI effects and the conditions for which the FSI are well understood. In addition, the use of light-cone kinematical variables will be introduced which facilitates the conservation of variables which are important for the extraction of the initial momentum of the correlated nucleon pair. In this section we also discuss in detail the competing effects which can mask the SRC signal and how we intend to deal with them.

2.3.1 FSI, 'Almost anti-parallel geometry' and light cone variables analysis.

Final state interactions (FSI) can mimic NN SRC event. This can happen if one of the outgoing protons scatters elastically from a neutron in the same nucleus at an angle such that the recoil neutron enters the neutron counters. In this case the actual momentum

($\tilde{p}_m$) that the proton had before scattering from the electron is not what we are measuring $\vec{p}_m = \vec{p}_f - \vec{q}$. As a result one cannot be certain that the condition $p_m \geq k_F$, really probes the high momentum components in the nuclear ground state wave function. It will also smear the correlation between the neutron and the target proton momenta.

An important feature of the kinematics we are considering (large Q^2, $p_f \geq 1\ GeV/c$) is the applicability of the eikonal appoximation for the rescattering. It means that small angle rescattering of GeV nucleons causes mainly transfer of momentum in the plane transverse to the direction of their high momentum (see [33, 34, 35]). This allows us to control, to some extent, the amount of FSI by selecting the angle between the target proton momentum and the incident virtual photon $\vec{q}$.

The best geometry for the suppression of FSI would be the parallel kinematics (see Fig. 8c). The large p_m and large q combine to a very large p_f which cannot be mimicked by FSI. Unfortunately, this geometry has some disadvantage. The large p_m and large q create a low x which entails contamination from resonance production.

In view of the above, we chose kinematics which we call 'almost anti-parallel' (see Fig. 8e) in which we look at high momentum target protons (300-500 MeV/c) that are almost anti-parallel to the $\vec{q}$ direction ($x > 1$). If they are fully correlated with another spectator nucleon and the pair is at rest, the spectator will be ejected at about 90 deg to the beam. This specific kinematical setup is a good compromise between the singles rates in the neutron counters (see section 3.2) and the suppression of FSI.

For light nuclei , $A \leq 16$, calculations of FSI diagrams within the generalized eikonal approximation Ref.[37] shows that in addition to $x > 1$, the condition:

$$|p_{mz} + \frac{q_0}{q} E_m| \geq k_F \tag{9}$$

will confine the rescattering with another nucleon to within short range. As a result the FSI will take place mainly with the nearby partner nucleon in the correlation. Thus, it will not spoil the SRC characteristics of the process.

In addition, we will use light cone variables for the analysis of the data because they are less sensitive to FSI effects, as follows. With the light cone momenta $p_{m\pm}, p_{s\pm}$ the cross section of the reaction was given in equation eq.(6). In our case the specific decay function we wish to measure is:

$$D(p_{m-} \approx 2m - p_{s-}, p_{m+} \approx (m^2 + {p_{ts}}^2/(2m - p_{s-}), \vec{p}_{tm} \approx \vec{-}p_{ts}) \tag{10}$$

The advantage of describing high energy transfer reactions ($q \geq 1\ GeV/c$) with light cone variables lies in the fact that, while E_m and $\vec{p}_m$ change due to FSI, the combination of p_m and E_m in the form of the p_{m-} (or $\alpha = p_{m-}/m$) survives the FSI[36, 37]. The accuracy of the conservation of p_{m-} is given by [37]:

$$\tilde{p}_{m-} - p_{m-} \approx \frac{Q^2}{2q^2} E_m, \tag{11}$$

where the $\tilde{p}_{m-}$ is the corresponding momentum of the target nucleon before the interaction. It follows from this equation that the conservation of p_{m-} improves with increasing energy.

Thus one might expect that the description of the SRC in terms of (E_m, p_m) could be complicated by FSI, while it will be preserved in terms of the p_{m+}, p_{m-} (or α) representation.

2.3.2 MEC, isobar contributions, large Q^2 and x> 1

It is difficult to isolate the effects due to nucleons at close proximity from those caused by NN effects such as meson exchange currents, isobaric currents and other long range correlations. Also, final state interactions (as discussed in the previous section) can mimic large nucleon momenta and the signature for SRC. High Q^2 is the best way to select the SRC. The sensitivity to short ranges increases as the virtuality of the photon increases. Competing two-body effects diminish as $1/Q^2$ and are also reduced for x> 1 (see [38, 39]). The FSI become less important at high Q^2 and become easier to deal with by using light cone variables. For quasi-elastic scattering the knocked out proton moves in the forward direction with high energy and the eikonal approximation can be used in the calculations. Also, the high energy of that proton makes it easy to distinguish it from the spectator correlated hadron.

Within the kinematics of quasi-free scattering, we represent in Fig.9 the relations between the initial momenta of the target nucleon and the Bjorken variable $x \equiv \frac{Q^2}{2mq_0}$ for different values of Q^2. Here $q_0 \equiv E_e - E'_e$ and $Q^2 = 4E_eE'_esin^2(\theta_e/2)$ are the transfered energy and squared four-momentum to the nucleus, E_e, E'_e are the energy of the initial and scattered electrons and θ_e is the angle of the scattered electrons with respect to direction of the initial electron.

One can see in Fig.9 that both the $x < 1$ (parallel geometry) and $x > 1$ (anti-parallel geometry) regions provide large values for the initial momentum of the interacting nucleon. Thus experiments which aim to study the high momentum components of the nucleon should explore one of these two regions.

Fig.9 also shows that in order to achieve some large target nucleon momentum, a larger Q^2 is needed for the $x > 1$ region. This was the reason why low energy experiments mainly explored the $x < 1$ region. However, all experiments in the region of $x < 1$ have the disadvantage of being near the inelastic threshold for pion production. This situation becomes more acute with increasing energy transfer. For example, for nuclei with $A \geq 12 - 16$ the broad Fermi distribution causes the inelastic contribution to be as high as 40% of the (e,e') cross section at $Q^2 = 2$ $(GeV/c)^2$, even at $x \approx 1$[7, 27]. The exclusiveness of the triple coincidence reaction of the proposed experiment reduces that contribution drastically.

All this leads to an exclusive measurement of three particles in coincidence in a region of high energy, high Q^2 and x> 1. We choose to pay the price of the small cross section at $x > 1$ in order to decrease contributions from resonance effects.

2.3.3 The selected kinematics for the measurement

The experiment we propose is a triple coincidence measurement of a fairly low cross section corresponding to a very elusive feature in nuclear physics. The third arm (in addition to the two permanent magnetic spectrometers) is an array of counters which, due to the heavy shielding, is not flexible to move. The above means that we have to carefully choose a single, optimized kinematical setup for the measurement. As we discussed in the previous sections, we choose a large incident energy, large Q^2, large target proton momentum, large x and 'almost anti parallel' geometry.

The proposed kinematical setup is shown in Fig 10 together with the range of kinematical variables we will be sensitive to. We propose to do the measurement at $Q^2 = 2\ (GeV/c)^2$ with enough statistics for exploring the tail up to 600 MeV/c. We also plan to make a measurement at $Q^2 = 2.7\ (GeV/c)^2$ to check the scaling and make sure that we really have the assumed QE behavior. The kinematical conditions for that measurement are shown in Fig. 11. This check at a second Q^2 value is important since it is required to ensure the 'FSI and MEC free situation'. This way can we check the quasi-elastic nature of the reaction by verifying that the cross sections scale as the known free cross sections.

3 Experimental considerations

3.1 Experimental set up

Hall C has two spectrometers which are used routinely for (e,e'p) coincidence measurements. Both the momenta of the electron and the proton are measured [40]. That is the 'standard' setup for this hall for which all the necessary equipment, including electronics and data acquisition are available. It is also reasonable to assume that by the time we will be able to do the experiment, also the off-line data analysis for the (e,e'p) part of the measurement will be working routinely .

The electron and proton spectrometers will be set according to the criteria we discussed in section 2. Fig. 12 shows the selected kinematics and the experimental set up.

To detect an eventual correlated neutron or proton, we will install a third arm detector similar to the one we used for the BNL experiment (see Appendix). We will use 24 plastic scintillators (100x10x12.5 cm^3) (from TAU and KSU). We plan to stack the detectors in an horizontal position with the center of the array at beam height. There will be 3 layers of 10 cm each, adding up to a depth of 30 cm in the direction of the target. The total area is $1 \times 1m^2$. At a distance of 3 meter from the target the array will cover a total angular range of about ± 10 deg. In front of the scintillators we will put 1/2 inch thick scintillators in order to separate charged and neutral particles.

All scintillators are available. A mounting frame will be built at KSU. We do not plan to move the counters during the run for angle changes. Shielding blocks which are available at TJNAF will be used to build a hut covering all sides except in the target direction. In front of the 1/2 inch scintillators we will place lead sheets sufficient to reduce the γ ray background but still allowing the detection of "third arm" protons above 400 MeV/c. The details of the shielding wi ll be decided on the basis of the rough background measurements we made parasitically, and which are discussed in the next section. We hope to perform more systematic background measurements in the near future, sufficiently early to plan the shielding on the basis of sound data.

Hall A also has all the facilities for performing this experiment. The larger momentum acceptance of the hadron spectrometer of hall C will save running time.

3.2 Parasitic background measurements in hall C.

Measurements were performed by Sudhir Malik (TAU) with the help from Steve Wood (TJNAF)and Eli Piasetzky (TAU). The measurements were done in November 1997 in a parasitic mode, in hall C during exp. 93-021 .

A schematic view of the experimental set up in hall C is shown in Fig 13. The counters were $12.5 \times 10 \times 30cm^3$ plastic scintillators with 2 inch PM's on both sides. The paddle was a $12.5 \times 30 \times 1cm^3$ plastic scintillators with one PM. The counters were shielded on top, front and back by 2 inches of Pb and below by 3 meter of concrete. There was no shielding on the sides.

The measured singles rates in counter 1 (left PM), in units of nucleon luminosity, are presented in table 3.I.

Table 3.1

run	energy(GeV)	SOS angle(deg)	current (μA)	target	rat./lum.[$10^{-36} cm^2$]
1	1.8	20	5.5	C 1mm	688
2	1.8	20	5.5	C 1mm	655
3	1.8	20	5.5	C 1mm	619
4	1.8	20	6.1	H 4cm	291
5	1.8	20	6.1	D 4cm	287
6	2.68	36.5	7.4	D 12cm	328
7	2.68	36.5	74	D 4cm	218
8	3.547	45.36	7	H 4cm	385
9	3.547	45.36	93.5	H 4cm	268
10	3.547	21.87	43.5	D 4cm	248

It seems that, within the relevant range, we can assume about a constant singles background of $(300) \times 10^{-36} cm^2$ for H/D. The measured carbon rates are about a factor of 2 higher.

If we assume that the BG is target-dominated and if we scale the results by the solid angles we get for a counter at 3 meter distance from the H/D target:

$rate/lum = (300 \times 10^{-36} cm^2) \times (5.3/3)^2 = 1000 \times 10^{-36} cm^2$

Thus, until we get new and systematic background results, we will work under the assumption that we have background rates of $2 \times (3 \times 10^{-33}) \times (nucleon\ luminosity)$ in a standard $12.5 \times 10 \times 100 cm^3$ counter at 3m from a C target.

3.3 Rates

For the purpose of estimating the counting rate we assumed that, at the high momenta we are focusing on (p_m=300-600 MeV/c), all counts are due completely to 2N SRC. We also assumed that under this condition the measured cross section can be expressed as

$$\frac{d\sigma}{dE_e d\Omega_e d\Omega_p} = K_0 \times a_2 \times Z \times \frac{d\sigma}{dE_e d\Omega_e d\Omega_{p_d}} \tag{12}$$

where $\frac{d\sigma}{dE_e d\Omega_e d\Omega_p}_d$ is the calculated deuteron differential cross section [41, 36, 42]. a_2 is a scaling ratio obtained from high Q^2 inclusive (e, e') scattering at $x > 1$ Ref.[7]:

$$a_2(^3He) = 1.7 \pm 0.3, \quad a_2(^4He) = 3.3 \pm 0.5 \quad a_2(^{12}C) = 5.0 \pm 0.5$$
$$a_2(^{27}Al) = 5.3 \pm 0.6 \quad a_2(^{56}Fe) = 5.2 \pm 0.9 \qquad a_2.(^{197}Au) = 4.8 \pm 0.7 \tag{13}$$

and K_0 is a kinematical factor related to the np-pair cm momentum in the nucleus. This factor is not well known and we used a conservative estimate of 0.2. Tables 3.2 and 3.3 give the estimated differential cross sections for $E_e = 4\ GeV$ at Q^2=2 and 2.7 $(GeV/c)^2$, respectively [42].

Another way to estimate the cross section for the proposed measurement is to rescale the lower energy measured cross section for exclusive deuteron disintegration from Ref.[43]. This experiment was done at approximately the same missing momenta as in the present proposal but with $Q^2 = 0.0377\ (GeV/c)^2$. To rescale this cross section to the region of $Q^2 \approx 2\ GeV^2$, we assume that, because of the cancelation between FSI and MEC contributions in the kinematics of Ref.[43], the PWIA calculation may describe fairly well the data [43]. Thus we use the factorized form of the PWIA approximation $\sim \sigma_{eN}\psi_D^2(p_m)$ and rescale the σ_{eN} to the kinematics of this proposal. For this we use the different off-shell models for σ_{eN} (see e.g. [44]). Within 20 % the results are the same for all the models used [42]. Taking the measured value $d\sigma/dEd\Omega_e d\Omega_p \approx 30pb/MeV/sr^2$ at $p_m \approx 500\ MeV/c$ and rescaling for σ_{eN} one obtains $\approx 0.06pb/MeV/sr^2$. Then taking into account the $z \cdot a_2 \approx 30$ factor one obtains $d\sigma/dEd\Omega_e d\Omega_p|_{Q^2=2\ (GeV/c)^2} \approx 1.8\ pb/MeV/sr^2$. This is the same value as shown in Table 3.2 which was obtained by the estimate based on the (e,e').

The ratio between the SRC np and pp pair contributions is not known and is one of the expected outcomes of the proposed measurement. For counting rate estimates we assume that $(np)/(pp)$ is between 4 (based on statistical isospin weight) and 7 (close to the photon data).

For the experimental acceptances and the proposed kinematical ranges we used the following values:

- $\Delta E_e = |E_e(p_s = 350MeV/c) - E_e(p_s = 250MeV/c)| = 50MeV$
- $\Delta\Omega_e = \Delta\Omega_{HMS} = 6msr$
- $\Delta\Omega_p = \Delta\Omega_{SOS} = 9msr$
- n detection efficiency = 0.3

The luminosity will be limited by the background singles rates on the plastic scintillators (the third arm). For a luminosity of $5 \times 10^{36} cm^{-2} sec^{-1}$ one can expect, according to section 3.2, a singles rate of $(6 \times 10^{-33}) \times (6 \times 10^{37}) \approx 0.4MHz$ on one $12.5 \times 10 \times 100 cm^3$ counter at 3 m from a C target.

In Tables 3.2 and 3.3, we present signal counting rates based on the above assumptions and for a luminosity of $5 \times 10^{36} cm^{-2} sec^{-1}$ (corresponding to 100 μA beam, a 1

mm thick C target) and the differential cross sections of columns 2. The total number of events for 150 hours of beam are shown in columns 3 for np pairs (n detected by the third arm) and in columns 4 for pp pairs(p detected by the third arm)

Table 3.2

$p_m[MeV/c]$	$\frac{d\sigma}{dE_e d\Omega_e d\Omega_p}$ (pb/sr^2MeV)	counts/150 hr (np pairs)	counts/150 hr (pp pairs)
300± 50	7.2	15000	7500-12000
400± 50	1.8	4000	2000-3500
500± 50	0.7	1500	700-1250

Table 3.3

$p_m[MeV/c]$	$\frac{d\sigma}{dE_e d\Omega_e d\Omega_p}$ (pb/sr^2MeV)	counts/150 hr (np pairs)	counts/150 hr (pp pairs)
300± 50	1.3	2700	1300-2200
400± 50	0.4	700	350-600

3.4 Requested beam time

The counting rates that are presented in Tables 3.2 and 3.3 lead to the following beam time request for preparations and the *two spectrometer setups*:

- Set up, establishing coincidences, calibrations, background checks: **100 hours**
- Measurements at $Q^2 = 2\ (GeV/c)^2$. About 20,000 (np) and 10,000-17,000 (pp) events in the $p_m = 300 - 500 MeV/c$ region and with a statistical accuracy of better than 4 percent at the highest ($500 \pm 50 MeV/c$) missing momentum bin.

  The kinematics are given in Fig.10 and the setup is in Fig.12a. **150 hours**
- Measurements at $Q^2 = 2.7\ (GeV/c)^2$. About 6,000 events. (Needed to establish the QE nature of the process by the appropriate expected scaling with the free cross section).

  The kinematics are given in Fig.11 and the setup is in Fig.12b. **150 hours**
- *TOTAL REQUESTED BEAM HOURS:* **400 hours**

3.5 Resources.

We summarize here the special resources needed for the experiment. These are in addition to the 'standard' hall C equipment for operating the two spectrometers, the beam and the target.

- 1. n- counters - The counters are available from KSU and Tel Aviv University.
- 2. veto counters - The detectors are available from KSU.
- 3. frame - will be built by KSU and TAU.
- 4. shielding - with TJNAF shielding blocks.
- 5. cables-We will need about 50 signal cables for the third arm counters. We also need about the same number of high voltage cables between the power supplies and the counters.
- 6. power supplies (50 channels) most likely to be supplied by KSU.
- 7. fast electronics - each of the detectors has 2PM's. The signals will go to CFD's. There will also be a few veto counters. We have the necessary CFD's. We also have the NIM units for the hardware trigger logic. The two PM's on each plastic bar are operated in coincidence after which all counters are also OR'ed. Thus, just one single signal will announce a hit in the third arm counter which can then be used to create a triple coincidence with a quasi-free event in the (e,e'p) reaction. The third arm counters will not be part of the main trigger!
- 8. Readout electronics: We will have to read approximately 50 TDC signals. A small change will be required in the 'standard' DAQ in order to read the extra TDC's.
- 9. Manpower: The group has much experience in :

  (e,e'p) measurements

  triple coincidence measurements

  neutron detection

  The group is sufficiently large and experienced to perform the proposed experiment. We note the participation of hall C personnel.

Appendix. The A(p,2p+n) experiment at BNL.

This proposed experiment is to some extent a follow up of an A(p,ppn) measurement we performed at BNL. The experiment (E850) was performed at the AGS accelerator at Brookhaven National Laboratory with the Exclusive Variable Apparatus (EVA) spectrometer [45, 46, 47, 48].

The high-momentum transfer quasi-elastic C(p,2p) reaction was measured near 90^o c.m. for 6 and 7.5 GeV/c incident protons, in a kinematically complete coincidence experiment. The three-momentum components of both high p_t final state protons were measured. The setup is drawn in Fig. 1. It shows the solenoidal cryogenic magnet with an axial field in the direction of the beam, entering from the left. The beam hit targets located near the center of the magnet and the two emerging protons were measured in a series of detectors.

Great care was taken to ensure the quasi-elastic scattering nature of the events. A small excitation energy of the residual nucleus (E_{miss}) was imposed in order to suppress events where additional particles could be produced in the process. Inelastic events that leaked into the data were subtracted. The procedures and results are described in Mardor et al. [49, 47]. In Fig. 2 we show the distributions of two of the three momentum components. The component p_{fz} is the component parallel to the beam direction and p_{fy} is one of the transverse components. The momenta were measured up to 250 MeV/c per component,(about 430 MeV/c for the total momentum). Also in Fig. 2 , we compare the measured momentum distributions to a simple independent particle Fermi motion distribution. A harmonic oscillator (HO) was used with parameters fitted to C from electron scattering data [50]. The HO calculation and the data in the figure are normalized to 1000 at the first bin. As can be seen clearly , the independent particle model fails substantially to describe the large momentum tails of the distribution. It seems that one is forced to invoke some short range correlation contributions.

In the same experiment, in addition to the quasi-elastic C(p,2p) reaction, we also measured the emerging neutrons . Referring back to Fig. 1, we see at the bottom a series of scintillation counters which measured the neutron momenta by Time Of Flight (TOF). The neutrons were detected in coincidence with the two emerging high momentum protons. In Fig. 3 we present a schematic picture of the setup for the neutron detection. Below the targets we placed a series of 16 scintillation bars covering an area of 0.8×1.0 m^2 and 0.25 m deep. They spanned an angular range of 102 to 125 degrees from the target. The TOF resolution of σ= 0.5 nsec corresponds to a momentum resolution of σ= 30 MeV/c at the highest momentum. A set of veto counters served to eliminate charged particles. Lead sheets were placed in front of the veto counters in order to reduce the number of photons entering the TOF spectrum. A clearly identified peak at about 3 nsec per meter flight path, due to remaining photons from the targets, was used for calibration and to measure the timing resolution. We applied a cutoff in the TOF spectrum at 6 nsec per meter flight path, keeping neutrons below 600 MeV/c, in order to eliminate any photons.

An example of a triple coincidence event which displays a NN SRC, is shown in Fig. 4. We show the transverse components $\mathbf{p}_t(p_1)$ and $\mathbf{p}_t(p_2)$ of the two outgoing high momentum protons as they were reconstructed in the trajectory analysis. The transverse momentum component of the struck target proton $\mathbf{p}_t(p) = \mathbf{p}_t(p_1) + \mathbf{p}_t(p_2)$ and the component of the neutron on the plane perpendicular to the beam are drawn as well. If the struck proton was correlated with a nearby neutron and the *pn* pair is at rest, the neutron will emerge in the direction opposite to that of the struck proton and with the same magnitude $\mathbf{p}(n)$= - $\mathbf{p}(p)$. If the correlation is of short range nature, we also expect both p(n) and p(p) to be above the Fermi sea level.

Most of the events measured do not have these ideal characteristics. The angular correlation is spread out due to limited experimental resolution, to center of mass motion of the *pn* pair in the nucleus and to final state interactions (FSI) of the outgoing protons. Notwithstanding the inevitable smearing of the angular correlation, we can extract information on the *np* correlation from our data by relaxing somewhat the stringent "back to back" requirement. None of the above effects is sufficiently large to prevent us from determining whether the momentum of the target proton pointed upwards or downwards. All the neutrons are detected in the downward direction. Consequently, we concentrate on the vertical (up-down) component of the struck proton. In Fig. 5 we plotted that component with respect to the *total momentum* of the neutron obtained from both the 5.9 and 7.5 GeV/c beam momenta. Each data point represents a single measured event. The resolution of the vertical momentum component depends on the azimuthal angle of the *pp* scattering plane. The resolution is best for a horizontal scattering plane and worst for the vertical plane. The different sizes of the error bars in Fig. 5 reflect this variation in the resolution.

Any proton with a vertical component in the downward direction cannot be a partner in the two-nucleon *np* correlation. We see that, up to a neutron momentum of $k_F \simeq 220$ MeV/c, (see the vertical dashed lines in Fig. 5) there are proton components in the downward as well as in the upward directions. Above that momentum there are very few downward pointing proton momenta and most point upwards. This is what one expects for correlated nucleon pairs. The large neutron momenta are associated with upward going protons while below the Fermi level, where the momenta can originate from the mean field, there is no preference. In order for neutrons to reach the counters below the targets they need some minimal downward component p_n^{vert}, which increases with the total neutron momentum. If the neutron is correlated with a proton, that proton will need an upward component which is equal in size to p_n^{vert}. The slanted dashed line in the figure represents this transverse momentum balance. All "correlated points " would lie on that line if there were no transverse motion of the *pn* pair nor FSI. Correlated neutrons with a larger downward component are associated with protons above that dashed line.

The absence of downward pointing proton momenta at high neutron momenta, is a clear indication of the dominance of two-nucleon correlations. We emphasize the fact that the conclusion is based on kinematics and does not depend on specific theoretical models.

A series of tests were performed to ascertain that the up/down asymmetry in Fig. 5. is not an experimental artifact of the spectrometer or of analysis procedures. We looked for asymmetries in, (i) the double coincidence $(p, 2p)$ quasi-elastic scattering data, (ii) the triple coincidence data, where the third coincidence was taken from the photon peak in the neutron counter and (iii), we changed the E_{miss} region to $1.2 < E_{miss} < 2$ GeV. We did not observe asymmetries in any one, or combinations, of these tests.

Final state interactions could, in principle, mimic this asymmetry. This can happen if one of the outgoing protons scatters elastically from a neutron in the same nucleus, at an angle such that the recoil neutron enters the neutron counters. The momentum transferred to the proton cannot be distinguished from the original momentum of the struck proton before the hard interaction. Since the neutron detectors are positioned at a backward angle (about 114 ± 12 deg), the probability for such a recoil neutron to enter the counters is very small. We estimated the FSI contribution to the events shown in Fig 5. in the following way. We assumed that the FSI can be described by a Glauber-like calculation, as in Ref [51]. We simulated the geometry of the spectrometer and neutron detectors and determined the number of neutrons and their momenta that could contribute to Fig.5, for all the $(p, 2p)$ quasi-elastic events. The contribution of FSI to the events in Fig.3 is about 3 above 220 MeV/c and about 2 below 220 MeV/c. The number of initial state interactions for the 6 GeV/c projectile, causing a neutron to recoil to an angle of 100 deg, is negligible.

In conclusion, even with limited statistics, it is possible to identify two-nucleon short range correlations on an event by event basis. The identification is based on kinematical arguments. The measured events are associated with high momentum components of the nuclear wave function. It seems that high energy exclusive reactions are an effective tool for the study of SRC in nuclei and it should encourage further studies, such as high energy $(e, ep + N)$ and more $(p, 2p + n)$ measurements.

During the experiment we collected only a very small fraction of the planned statistics due to frequent breakdowns in the cryogenic magnet. The magnet has now been repaired. We plan to upgrade the experimental setup at BNL and improve the statistics by two orders of magnitude. We also plan to detect neutrons over a larger phase space range, inparticular we wish to cover larger angles with respect to the incident beam. The new data will enable us to make quantitative statements about the fraction of two-nucleon short range correlations in the large momentum tail as a function of the target nucleon momentum. We will also use a variety of nuclear targets in order to check any possible A dependence. The results will be extremely valuable for the understanding of the NN interaction at all distances.

References

[1] C. Ciofi degli Atti, E. Pace and G. Salme, Phys. Rev. **C21**, 805 (1980).

[2] O. Benhar, A. Fabrocini and S. Fantoni, Nucl. Phys. **A505**, 267 (1989).

[3] C. Ciofi degli Atti, L. Frankfurt, S. Simula and M. Strikman, Phys. Rev. **C44** 7 (1991).

[4] V.Pandharipande, I.Sick and P.K.A. de Witt Huberts, Rev. Mod. Phys. 69(1997), 981.

[5] D.B.Day *et al.*, Phys.Rev.Lett. 59, 427 (1987).

[6] D.Potterveld, Proceedings, PANIC 1996, p.155.

[7] L. L. Frankfurt, M. I. Strikman, D. B. Day and M. M. Sargsyan, Phys. Rev. **C48**, 2451 (1993).

[8] O. Benhar,et al. Phys.Rev.C47(1993),2218.

[9] J. S. O'Connell et al., Phys. Rev. Lett. **53**, 1627 (1984); Phys. Rev. **C35**, 1053 (1987).

[10] W.Bertozzi, R.W. Lourie and E.J. Moniz, in Modern Topics in Electron Scattering, (World Scientific, 1991), B.Frois and I.Sick eds.

[11] P.E.Ulmer *et al.*, Phys. Rev. Lett. 59, 1159 (1987).

[12] J. Koch and N. Ohtsuka, Nucl. Phys. **A435**, 765 (1985).

[13] G.van der Steenhoven *et al.*, Nucl.Phys. A484, 445 (1988).

[14] J.M. Le Goff et al., Phys. Rev. **C50** 2278 (1994).

[15] C. Marchand, et al., Phys. Rev. Lett. **60**, 1703, (1988).

[16] J.J. van Leeuwe, et al., *Talk given at the 15th International Conference on Few-Body Problems in Physics (FB 97), Groningen, Nederlands, 22-26 Jul 1997.* nucl-ex/9709007.

[17] C.J.G.Onderwater *et al.*, Phys. Rev. Lett. 78, 4893 (1997).

[18] L.J.H.M.Kester *et al.*, Phys. Rev. Lett. 74, 1712 (1995).

[19] R.Ent *et al.*, Phys. Rev. Lett. 62, 24 (1989).

[20] A.Zondervan *et al.* Nucl. Phys. A587, 697 (1995).

[21] J.Arends *et al.*, Z.Physik A298, 103(1980).

[22] M.Kanazawa *et al.*, Phys.Rev. C35, 1828 (1987).

[23] Yu D.Bayukov *et al.*, Sov. J. Nucl. Phys. 42, 116 (1985), and 238; Sov. J. Nucl. Phys. 34, 437 (1981).

[24] K. Egiyan et al., submitted to Physics of Atomic nuclei, 1997.

[25] E. Matsinos et al., Z.Phys. **C44**, 79 (1989).

[26] D.Ashery and J.P.Schiffer, Ann. Rev. Part. Sci. 36, 207 (1986).

[27] D. Day and B. Filippone (spokespersons), CEBAF proposal E-89-008.

[28] J. Zhao (spokesperson), TJNAF proposal E-97-011.

[29] K. Egiyan (Spokesperson), CEBAF proposal E-89-036.

[30] S. E. Kuhn and K. A. Griffioen (spokespersons), CEBAF proposal E-94-017.

[31] H. Begahai (spokesperson), CEBAF proposal E-89-015.

[32] V. Gavrilov and G. Leksin (spokespersons), CEBAF proposal E-89-032.

[33] R. J. Glauber, in *Lectures in Theoretical Physics*, edited by W. Brittain and L. G. Dunham, Wiley Interscience, New York, **V.1**(1959).

[34] E.J. Moniz and G.D. Nixon, Annals of Physics **67** 58 (1971).

[35] D.R. Yennie in *Hadronic Interactions of electrons and Photons* ed. J. Cummings, D. Osborn, 321 (1971).

[36] L. L. Frankfurt, W. G. Greenberg, J. A. Miller, M. M. Sargsyan and M. I. Strikman, Z. Phys. **A352**, 97 (1995).

[37] L. L. Frankfurt, M. M. Sargsyan and M. I. Strikman, Phys. Rev. **C56**, 1124 (1997).

[38] R. G. Arnold et al., Phys. Rev. **C42** (1990),R1.

[39] J. M. Laget, Phys. Lett. **B199**, 493 (1987).

[40] D. Geesaman (spokesperson), CEBAF proposal E-91-013.

[41] K.Sh. Egiyan, M.M. Sargsyan, "Cross-Section of Electron - Off-Shell Nucleon Interaction" CEBAF-PR-93-001, (1993).

[42] M. Sargsyan, private communication.

[43] S. Turck-Chieze, P. Barreau, et al., Phys.Lett.142B(1984),145.

[44] T. de Forest, Nucl Phys. **A392**, 232 (1983).

[45] M.A.Shupe *et al. EVA, a solenoidal detector for large angle exclusive reactions: Phase I - determining color transparency to 22 GeV/c.* Experiment E850 Proposal to Brookhaven National Laboratory, 1988 (unpublished).

[46] *Measurement of the dependence of the $C(p, 2p)$ cross section on the transverse component of the spectral momentum*, S.Durrant, PhD thesis, Pennsylvania State University, 1994 (unpublished).

[47] *Quasi-Elastic Hadronic Scattering at Large Momentum Transfer*, Y.Mardor, PhD thesis, Tel Aviv University, 1997 (unpublished).

[48] J.Y.Wu *et al.* , Nuclear Instruments and Methods A 349 (1994) 183.

[49] Y.Mardor *et al.*, preprint nucl-ex/9710002 16 Oct, 1997.

[50] M. Sargsyan, private communication, and H. Bidasaria et al. Nucl. Phys. A355, 349 (1981).

[51] I.Mardor *et al.*, Phys. Rev. C46, 761 (1992).

Figure Captions

Fig. 1 Cross section of the EVA detector at BNL. The detector has cylindrical symmetry around the beam axis. The magnetic field lines emerging from the downstream end of the solenoid are collected and returned through the large iron plug. The scale in the figure is in centimeters. The C's are cylindrical drift chambers and the H's are scintillator hodoscopoes.

Fig. 2 P_{fz} is the longitudinal momentum distribution, obtained from the α distributions measured at 6 and 7.5 GeV/c and corrected for the s dependence induced by the elementary free cross section. $|P_{fy}|$ is the transverse distribution, obtained from the measured transverse distributions. HO is a harmonic oscillator independent particle model calculation. The P_{fz} and HO distributions are normalized to 1000 at the first bin. A model dependent SRC distribution [42] is shown, arbitrarily normalized, just to show the shape.

Fig. 3 The neutron counter set up. The z axis is the symmetry axis of the EVA spectrometer. The spectrometer itself is not shown. θ_{min}=102 ^{o} and θ_{max} = 125 ^{o}.

Fig. 4 A triple coincidence event measured at an incident momentum of 5.9 GeV/c. The vectors are projections on the plane normal to the incident beam. The axes are the vertical and horizontal directions in that plane. The $\mathbf{p}_t(p_1), \mathbf{p}_t(p_2)$ are the transverse momenta of the outgoing protons, $\mathbf{p}_t(p)$ is the transverse momentum of the target proton before the interaction and $p_t^{vert}(p)$ is its vertical component. $\mathbf{p}_t(n)$ is the projection of the neutron momentum on the same plane. The circle indicates the scale for a momentum of 220 MeV/c.

Fig. 5 The vertical component of the target nucleon momentum vs. the total neutron momentum.The positive vertical axis is the upward direction. The events shown are for triple coincidences of the neutron with the two high energy protons emerging from the QE $C(p, 2p)$ reaction. The squares are for the 5.9 GeV/c incident beam and the triangles are for 7.5 GeV/c. The dashed lines are explained in the text. We associate the events in the upper right corner with NN SRC.

Fig. 6 Breakup of NN SRC in the nucleus induced by a virtual photon.

Fig. 7 Diagram for the quasi-elastic breakup reaction of a pair at rest in the nucleus. The kinematical variable are defined in the text.

Fig. 8 Relative geometry between the target proton momentum and the incident virtual photon momentum $\vec{q}$. a,b- perpendicular, c-parallel, d-antiparallel, e-'almost antiparallel'.

Fig. 9 The x dependence of missing momentum p_m (in (GeV/c)) probed in $(e,e'p)$ reaction at different Q^2 = (0.5, 1, 2, 3, 4 *and* 5 $(GeV/c)^2$). The momentum of of the final proton $\vec{p}_f$ is parallel to $\vec{q}$.

Fig. 10 Kinematics for the reaction (e,e'p+N) in 'almost-parallel geometry' at Q^2 = 2.0 $(GeV/c)^2$. The variables are defined in the text. The table shows the values of these variables for p_m=300 and 500 MeV/c.

Fig. 11 Same as Fig 9. but for $Q^2 = 2.7$ $(GeV/c)^2$.

Fig. 12 Experimental set up for (e,ep+N) measurement at the selected kinematical conditions for $Q^2 = 2$ $(GeV/c)^2$ (a) and for $Q^2 = 2.7(GeV/c)^2$ (b).

Fig. 13 A schematic view of the set up used to measure the background in hall C.

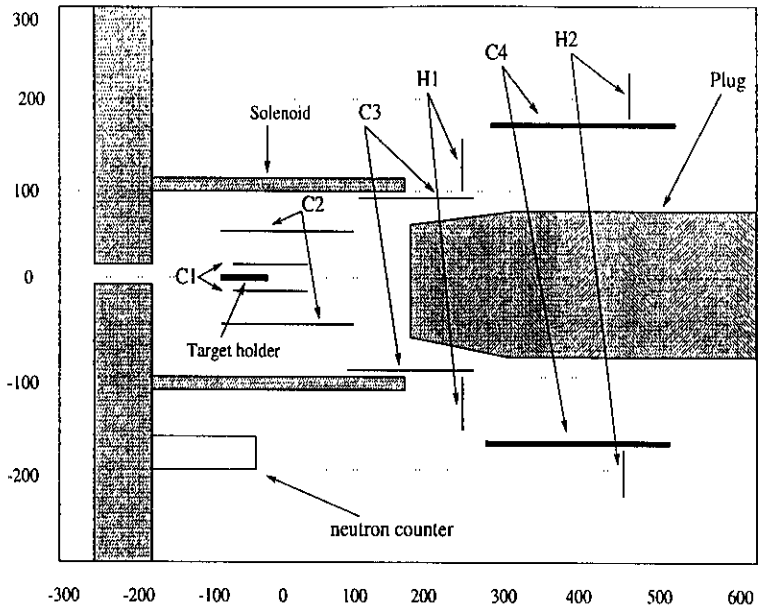

Figure 1

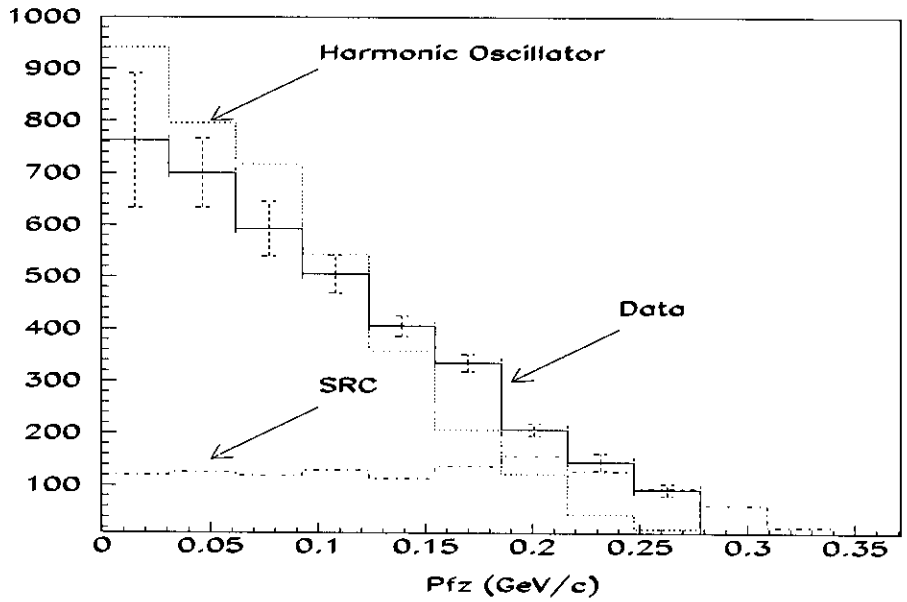

Figure 2

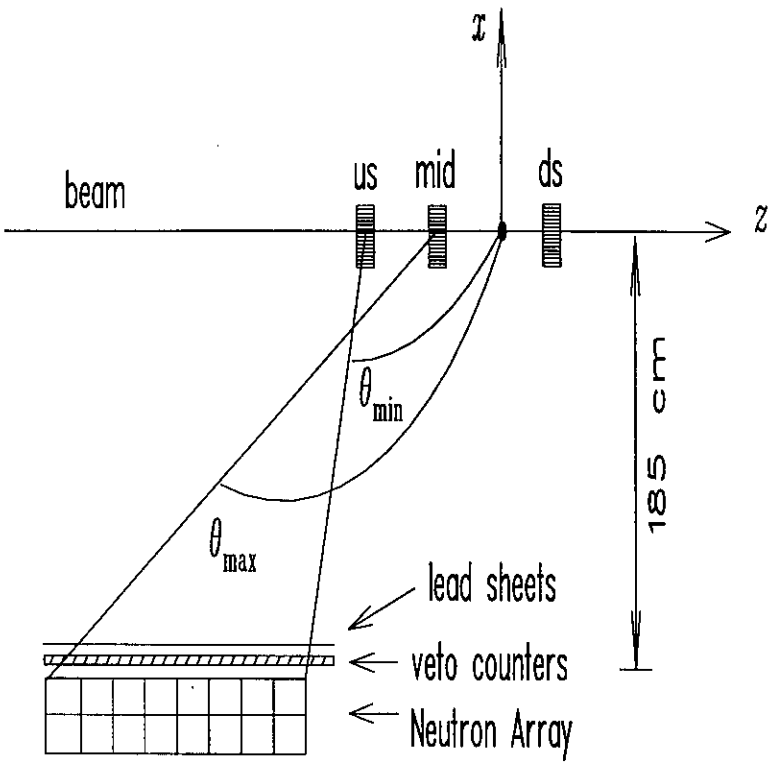

Figure 3

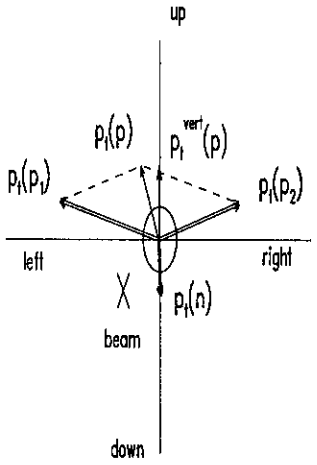

Figure 4

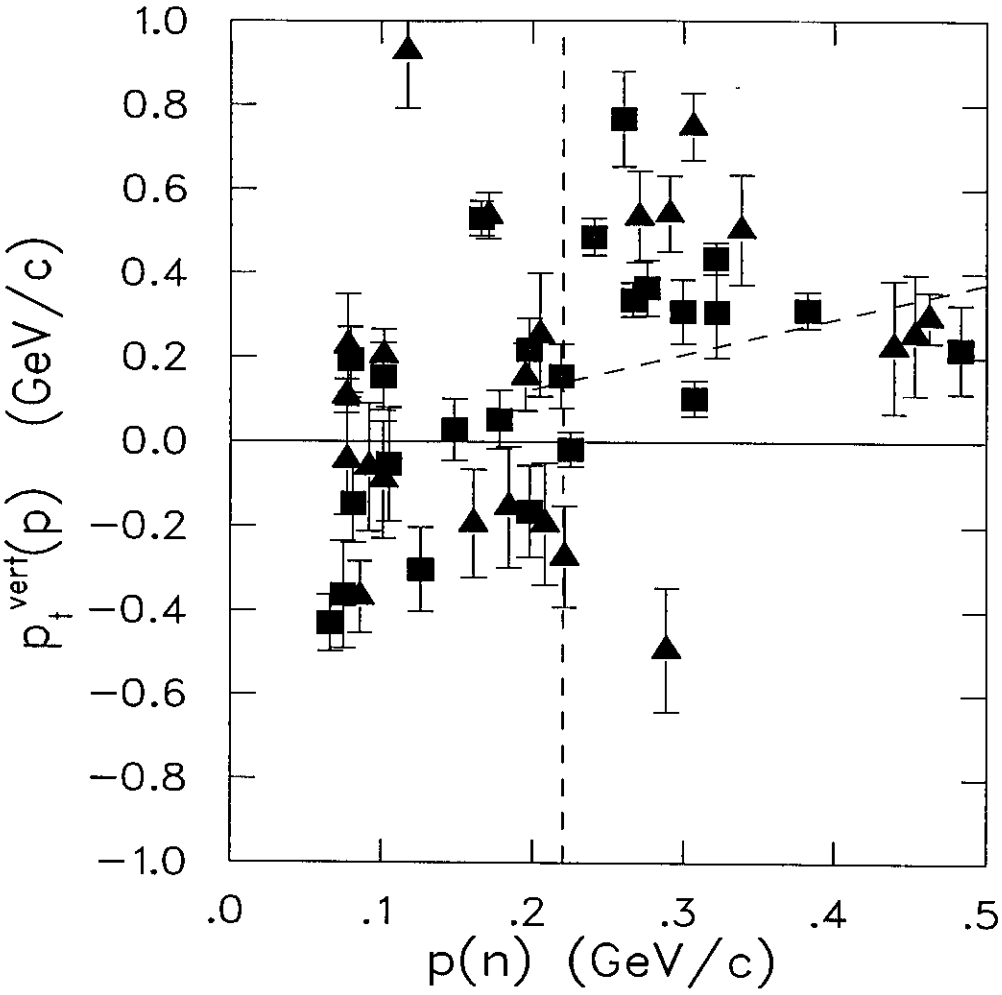

Figure 5

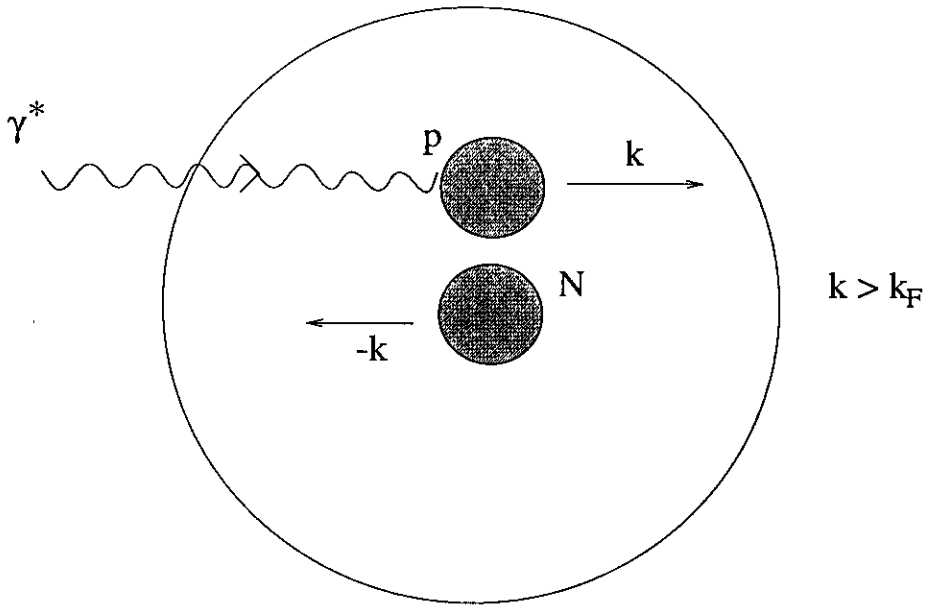

Figure 6

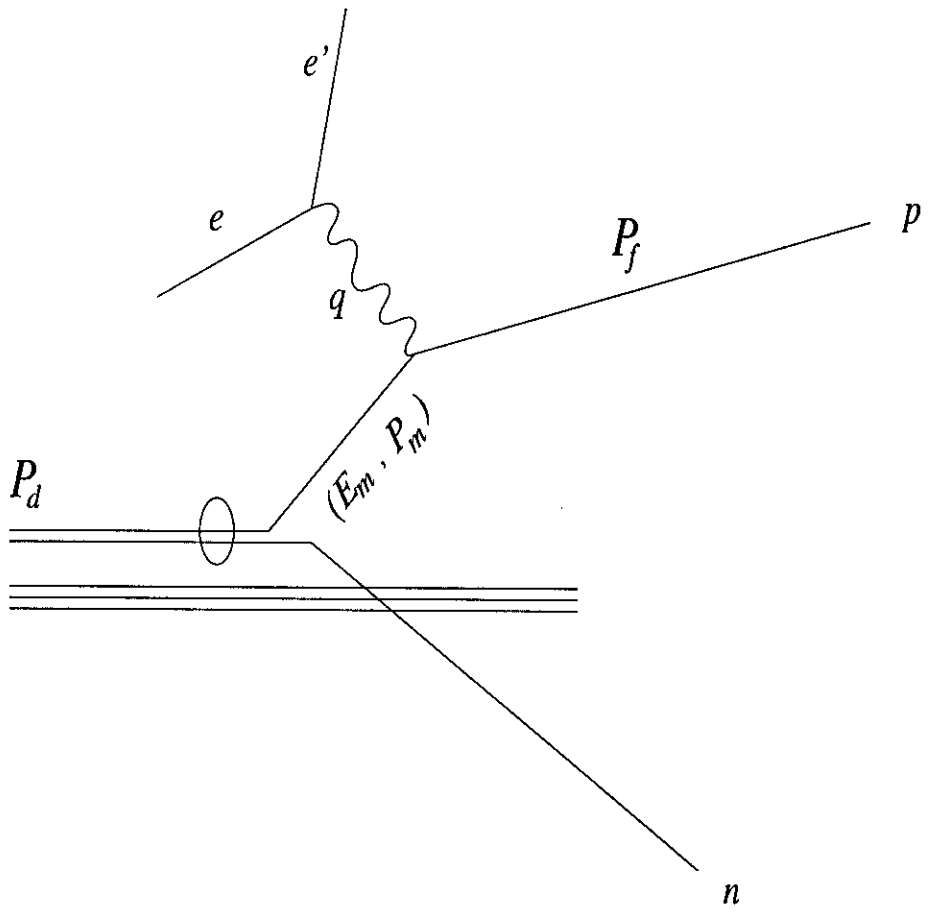

Figure 7

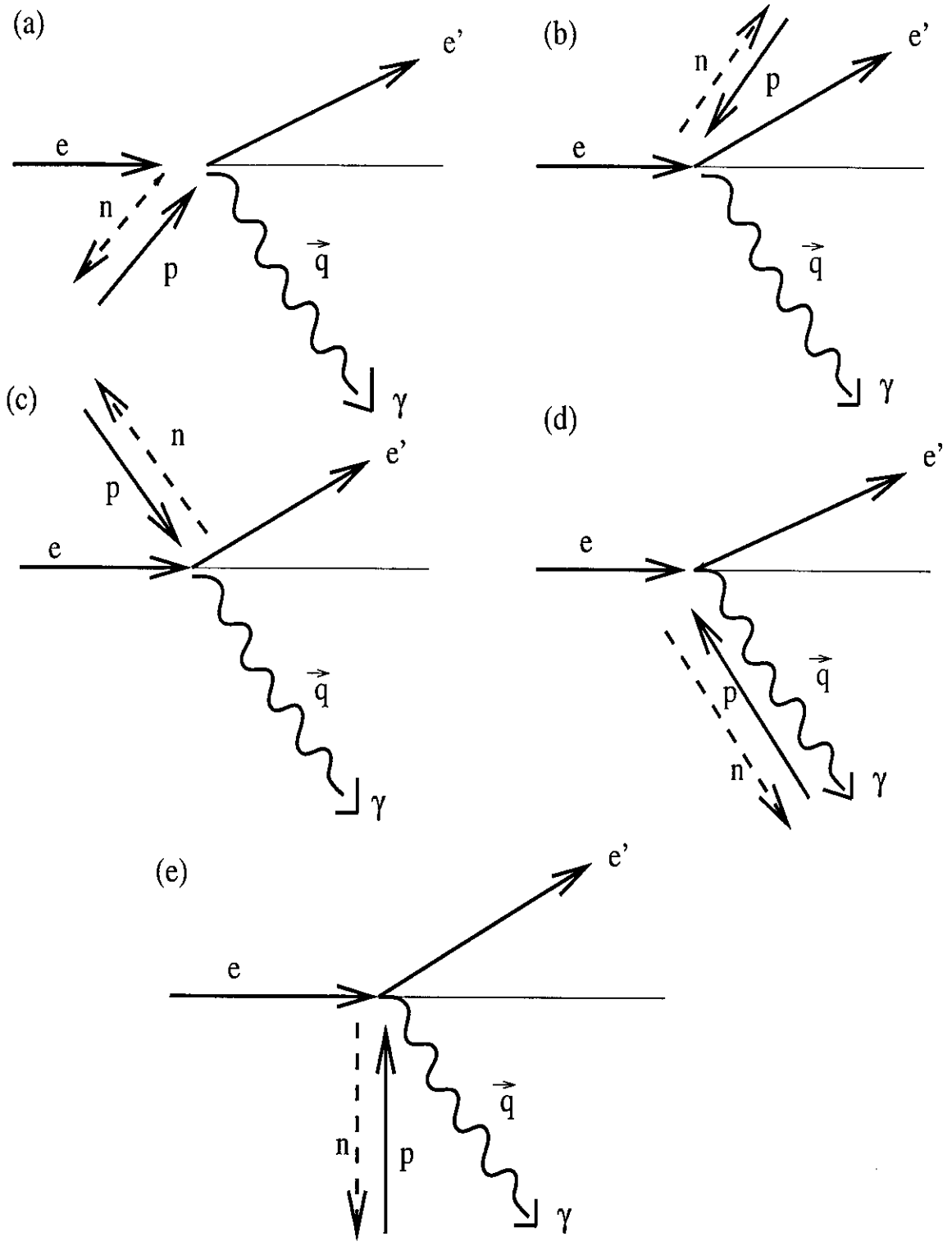
(a)
e'
e
n
p
$\vec{q}$
γ
(b)
e'
n
p
e
$\vec{q}$
γ
(c)
n
p
e'
e
$\vec{q}$
γ
(d)
e'
e
$\vec{q}$
p
n
γ
(e)
e'
e
$\vec{q}$
n
p
γ

Figure 8

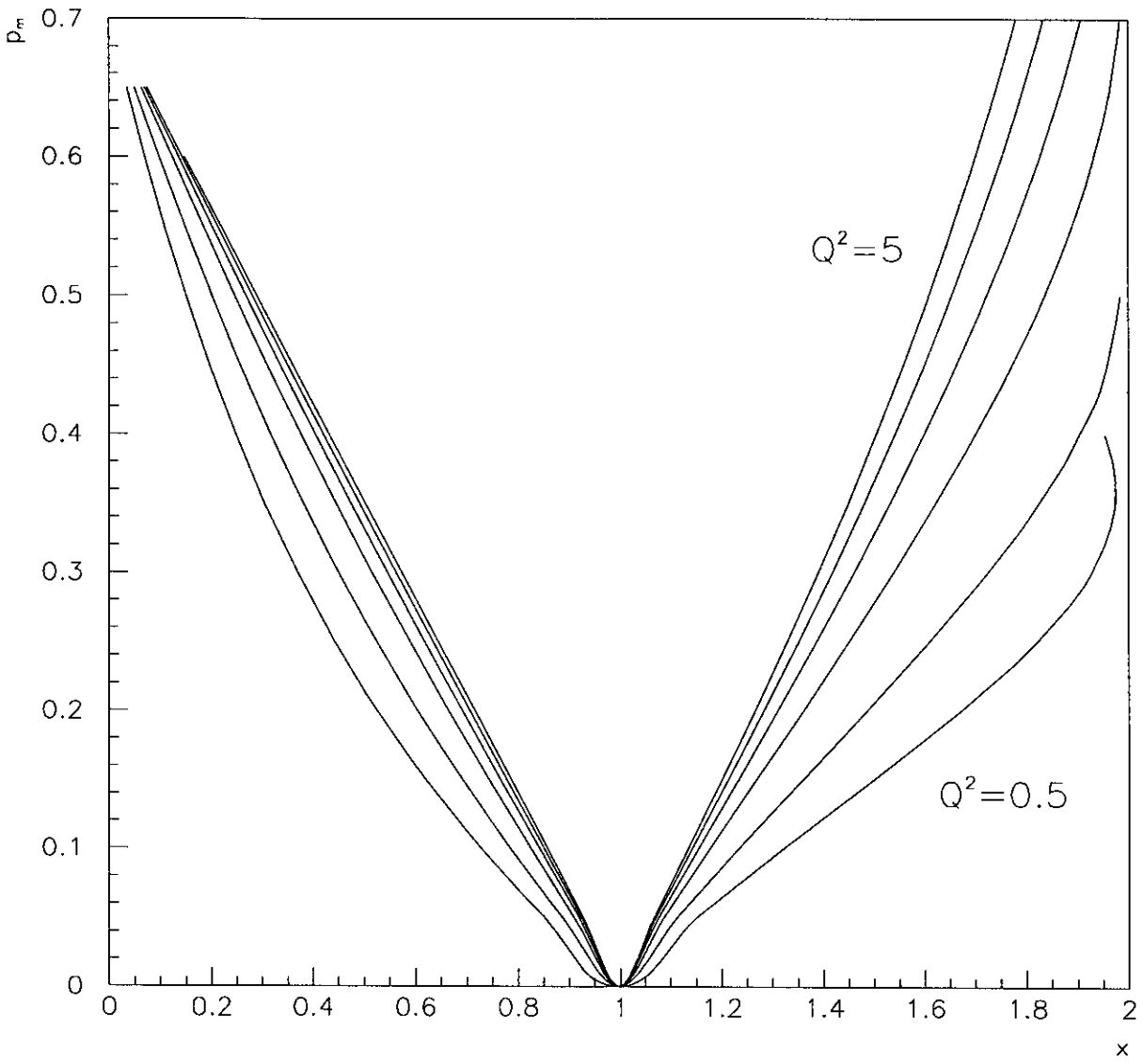

Figure 9

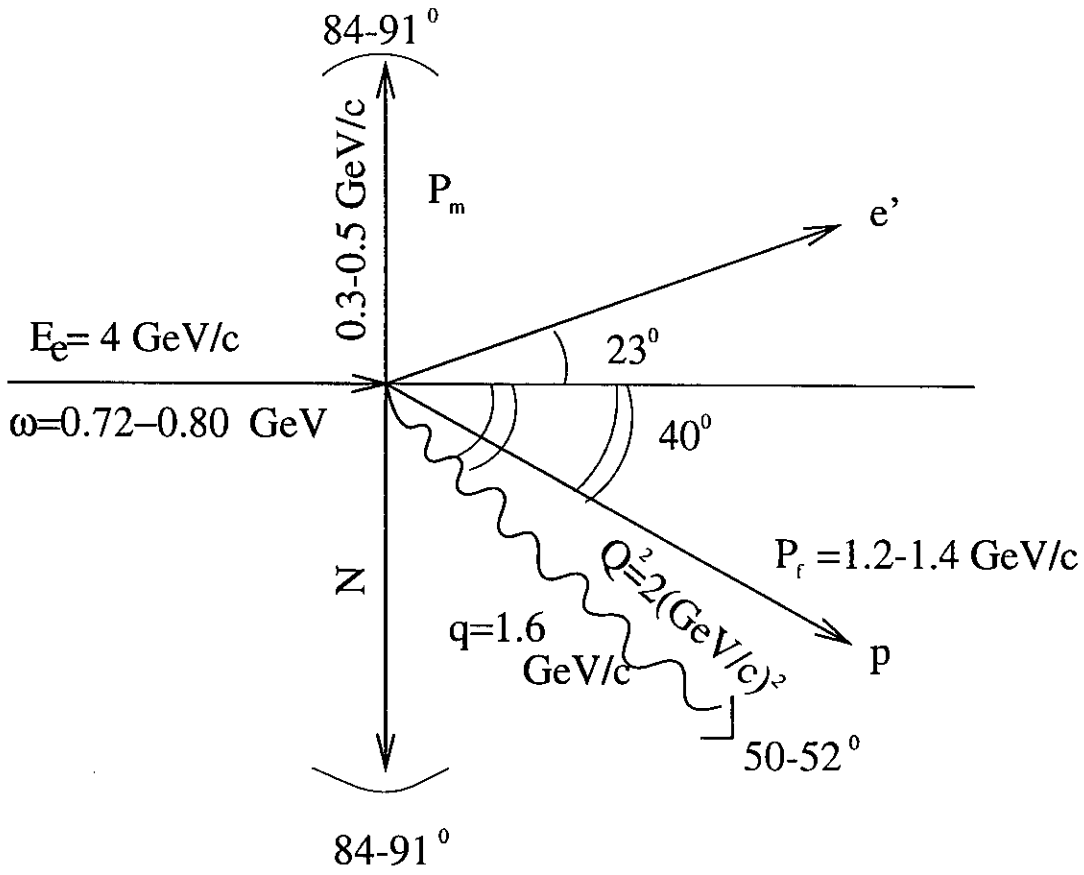

E_e =initial electron energy = 4 GeV

θ_e = scattered electron angle = 23^0

θ_N = spectator angle = 85^0

ϕ_N = azimuthal angle of spectator nucleon = 180^0

ω GeV	q GeV/c	Q^2 $(GeV/c)^2$	x	θ_q deg	P_f GeV/c	E_m GeV	P_m GeV/c	θ_p deg	ϕ_p deg
0.73	1.62	2.08	1.52	52.23	1.21	0.14	0.52	38.80	180.0
0.80	1.64	2.01	1.36	49.86	1.41	0.04	0.29	43.16	180.0

Figure 10

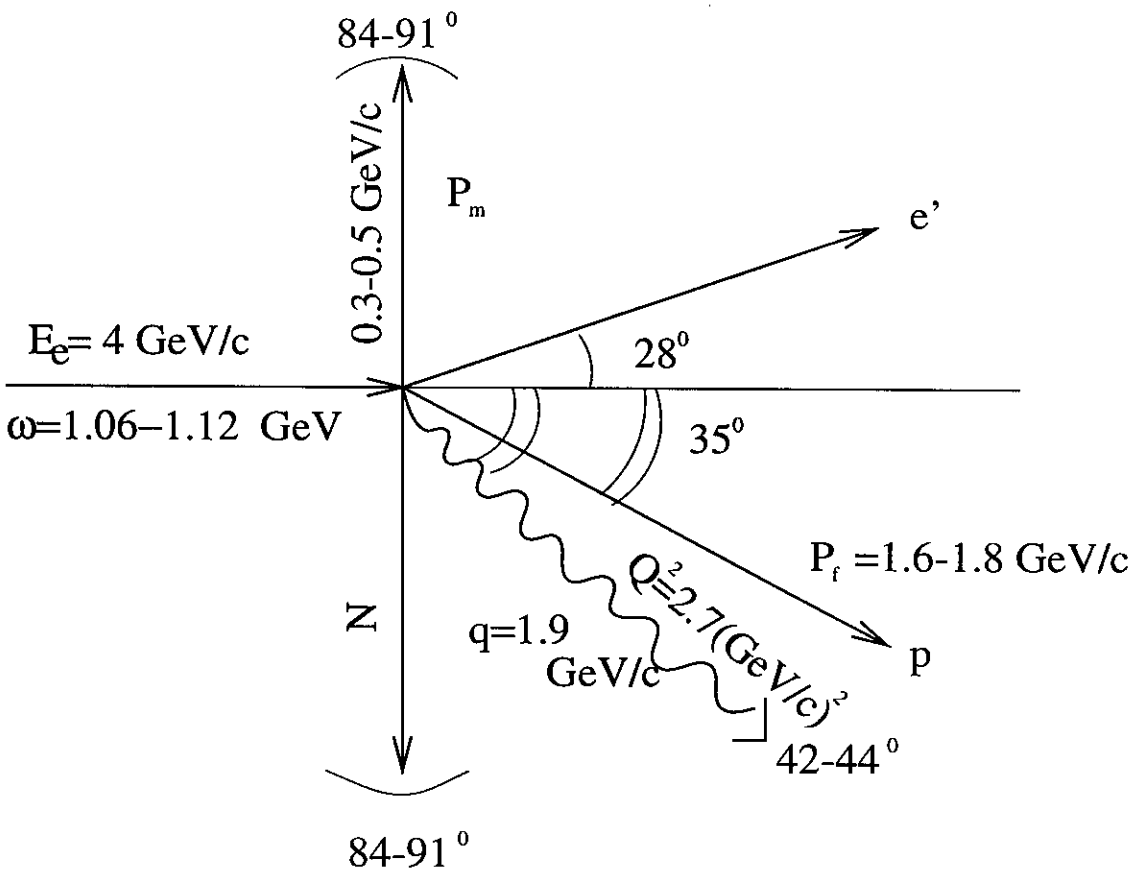

E_e =initial electron energy = 4 GeV

θ_e = scattered electron angle = 28^0

θ_N = spectator angle = 85^0

ϕ_N = azimuthal angle of spectator nucleon = 180^0

ω GeV	q GeV/c	Q^2 $(GeV/c)^2$	x	θ_q deg	P_f GeV/c	E_m GeV	P_m GeV/c	θ_p deg	ϕ_p deg
1.06	1.97	2.75	1.38	44.51	1.61	0.13	0.52	32.43	180.0
1.12	1.99	2.70	1.28	42.86	1.78	0.05	0.30	36.36	180.0

Figure 11

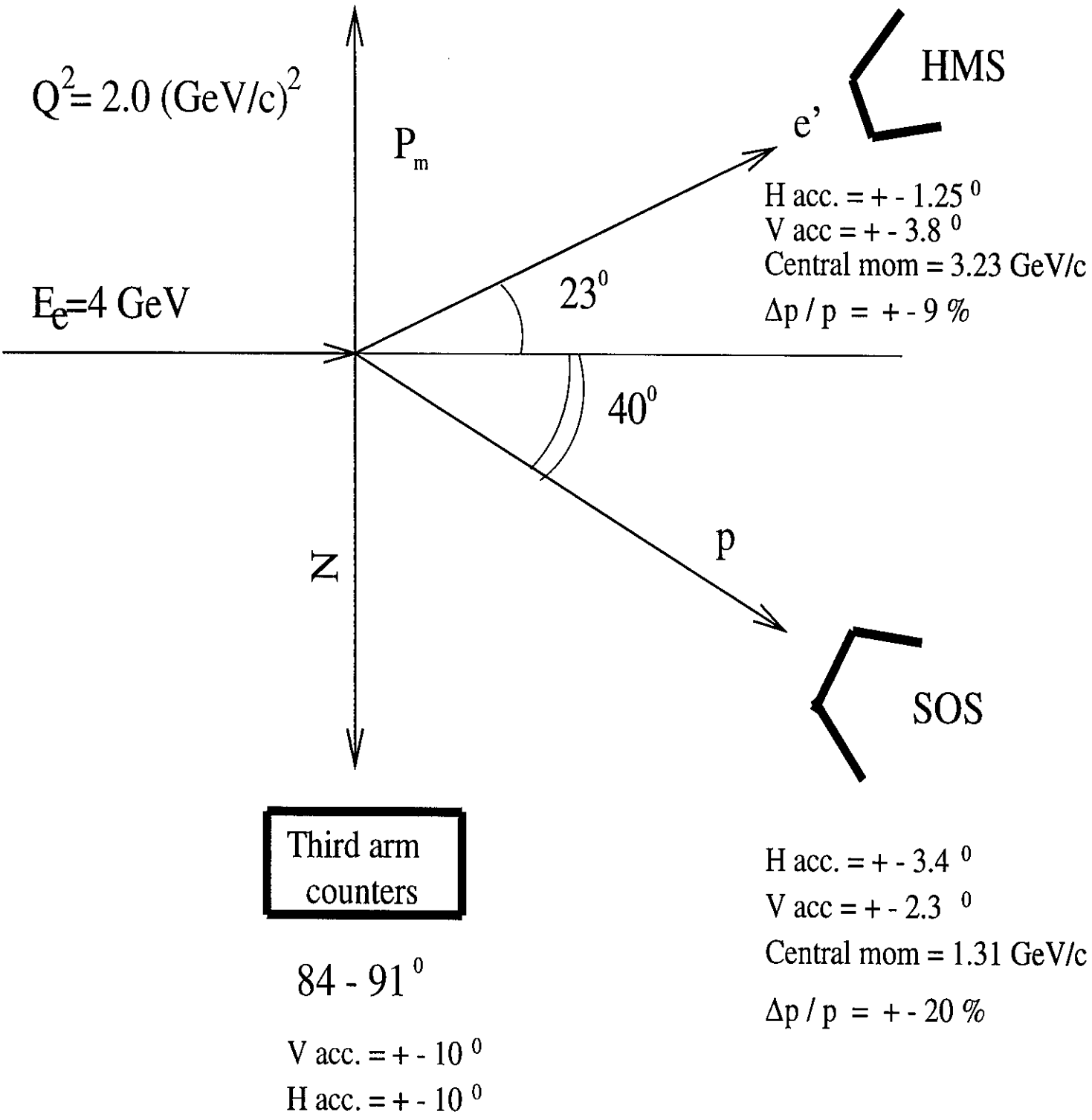
Q^2= 2.0 (GeV/c)^2
P_m
HMS
e'
H acc. = + - 1.25 ^{0}
V acc = + - 3.8 ^{0}
Central mom = 3.23 GeV/c
$\Delta p / p$ = + - 9 %
E_e=4 GeV
23^0
40^0
p
Z
SOS
Third arm counters
84 - 91 ^{0}
V acc. = + - 10 ^{0}
H acc. = + - 10 ^{0}
H acc. = + - 3.4 ^{0}
V acc = + - 2.3 ^{0}
Central mom = 1.31 GeV/c
$\Delta p / p$ = + - 20 %

Figure 12 a

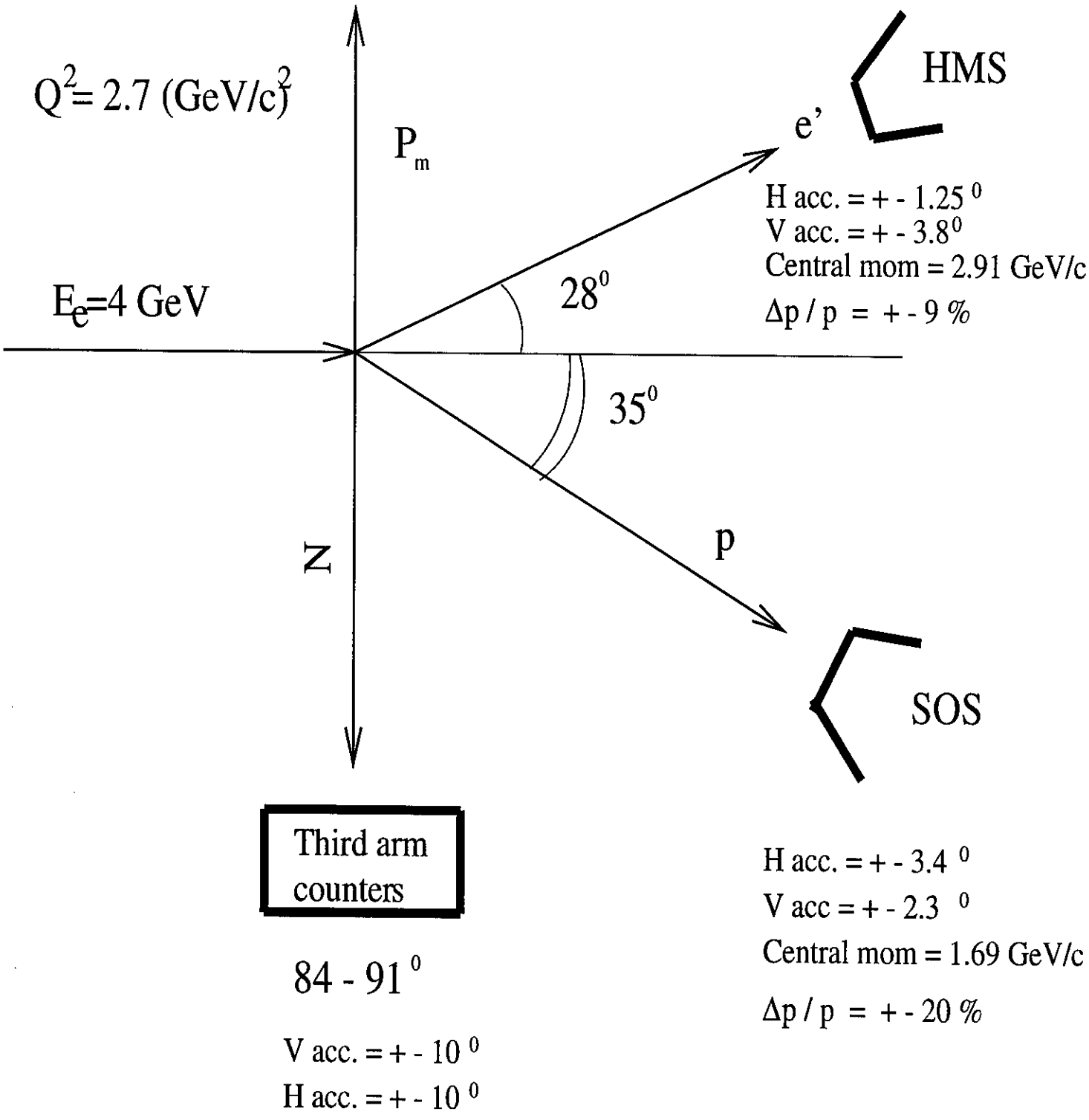
Q^2= 2.7 (GeV/c)^2
P_m
HMS
e'
H acc. = + - 1.25 ^{0}
V acc. = + - 3.8^0
Central mom = 2.91 GeV/c
$\Delta p / p$ = + - 9 %
E_e=4 GeV
28^0
35^0
N
p
SOS
Third arm counters
84 - 91 ^{0}
V acc. = + - 10 ^{0}
H acc. = + - 10 ^{0}
H acc. = + - 3.4 ^{0}
V acc = + - 2.3 ^{0}
Central mom = 1.69 GeV/c
$\Delta p / p$ = + - 20 %

Figure 12 b

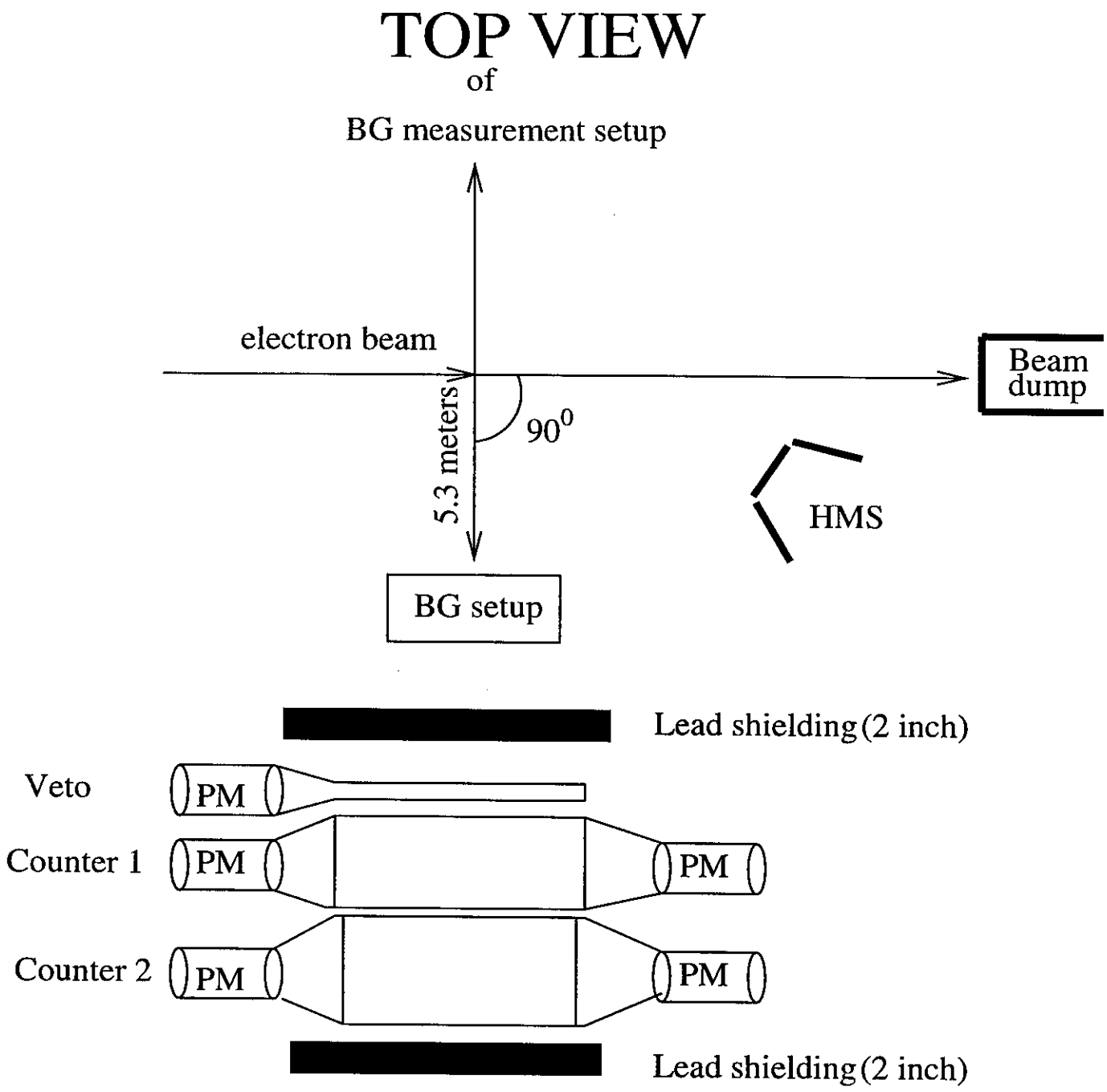

Shielding from top = 2 inch of lead
Bottom shielding = 3 meters of concrete
PM - Photomultiplier tube

Figure 13